Electronic Supplementary Material (ESI) for Journal of Materials Chemistry B.

Instant Hydrogelation Encapsulates Drug onto Implants Intraoperatively against Osteoarticular Tuberculosis

Yuan Li [a, b, #], Litao Li [b, #], Xiaoling Sha [a, b], Kuo Zhang [a], Guang Li [a, b], Yiguang Ma [a, b], Jin Zhou [c], Yanfei Hao [d], Zhong Zhang [e], Xu Cui [b, *], Pei-Fu Tang [b, *], Lei Wang [a, *], Hao Wang [a, *]

[a] CAS Center for Excellence in Nanoscience, CAS Key Laboratory for Biomedical Effects of Nanomaterials and Nanosafety, National Center for Nanoscience and Technology (NCNST), No. 11 Beiyitiao, Zhongguancun, Beijing 100190, China

E-mail: wanglei@nanoctr.cn, wanghao@nanoctr.cn

[b] Department of Orthopedic Medicine, The 4th Medical Center of Chinese PLA General Hospital, No. 51 Fucheng Road, Beijing 100000, China

Email: cuixuprossor@163.com, pftang301@163.com

[c] CAS Key Laboratory of Standardization and Measurement for Nanotechnology, CAS Center for Excellence in Nanoscience, National Center for Nanoscience and Technology (NCNST), No. 11 Beiyitiao, Zhongguancun, Beijing 100190, P. R. China

[d] The 8th Medical Center of Chinese PLA General Hospital, No. 17 Heishanhu Road, Beijing 100091, China

[e] CAS Center for Excellence in Nanoscience, CAS Key Laboratory of Nanosystem and Hierarchical Fabrication, National Center for Nanoscience and Technology (NCNST), No. 11 Beiyitiao, Zhongguancun, Beijing 100190, China

[#] These authors contributed equally to this work.

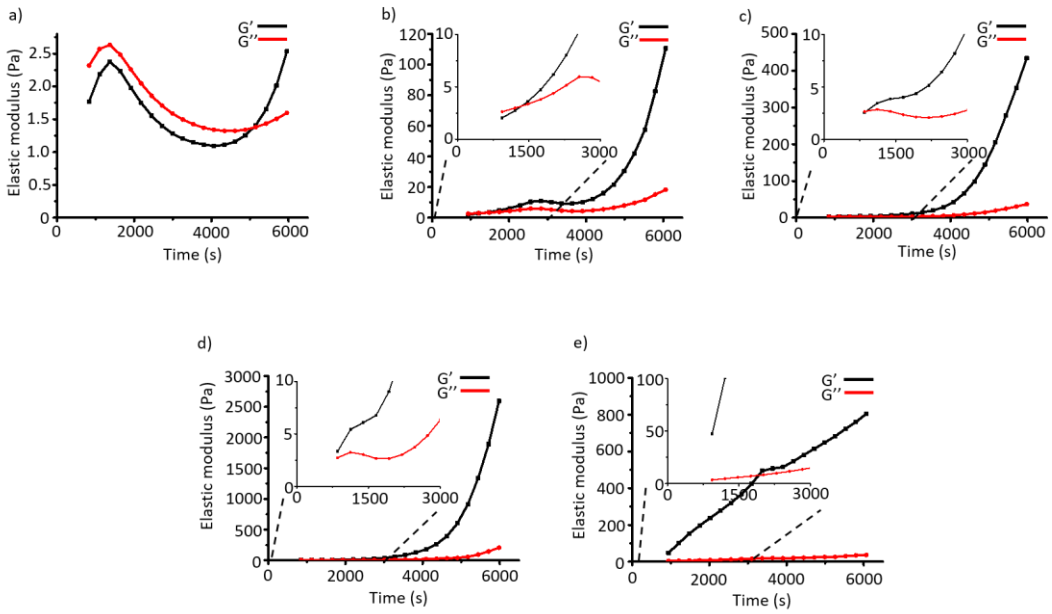

Figure S1. Optimization of the mass ratio of CS and β-GP. Rheological properties of CS/β-GP at 37 ºC in the condition of a) CS: β-GP, w/w, 1:7, b) CS: β-GP, w/w, 1:8, c) CS: β-GP, w/w, 1:9, d) CS: β-GP, w/w, 1:11 and e) CS: β-GP, w/w, 1:12.

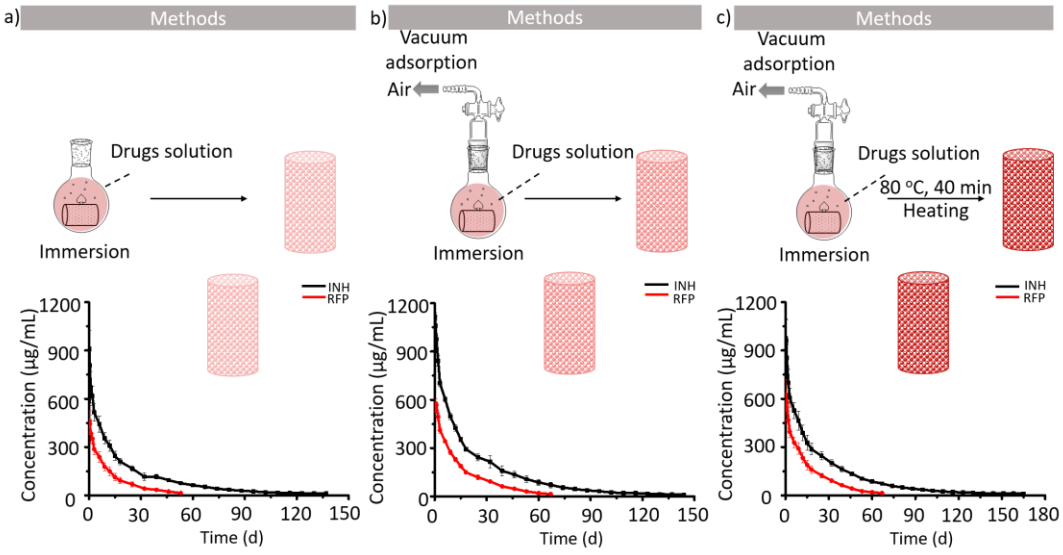

Figure S2. Optimization of the way of constructing DDSs (One-layer coating strategy). The methods of construction and its drug-release profile, respectively. The way of a) immersing, b) immersing and vacuum absorption and c) immersing, vacuum absorption and heating.

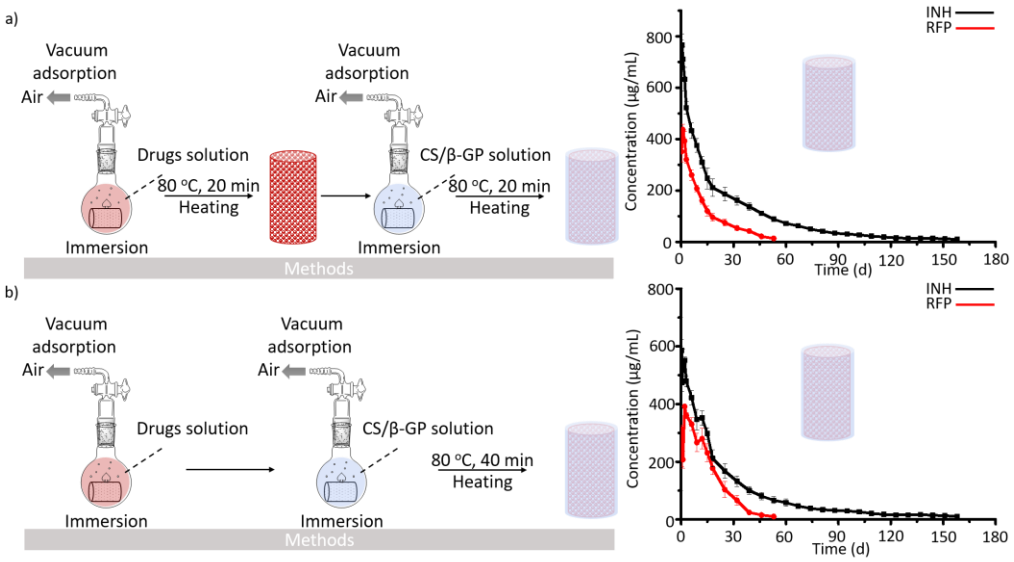

Figure S3. Optimization of the way of constructing DDSs (Two-layer coating strategy, i.e. encapsulating technology). The methods of construction and its drug-release profile in the way of a) heating scaffold with one layer coating for 20 min, followed by hydrogel layer coating and 20 min heating; b) heating scaffold with two layers coating for 40 min.

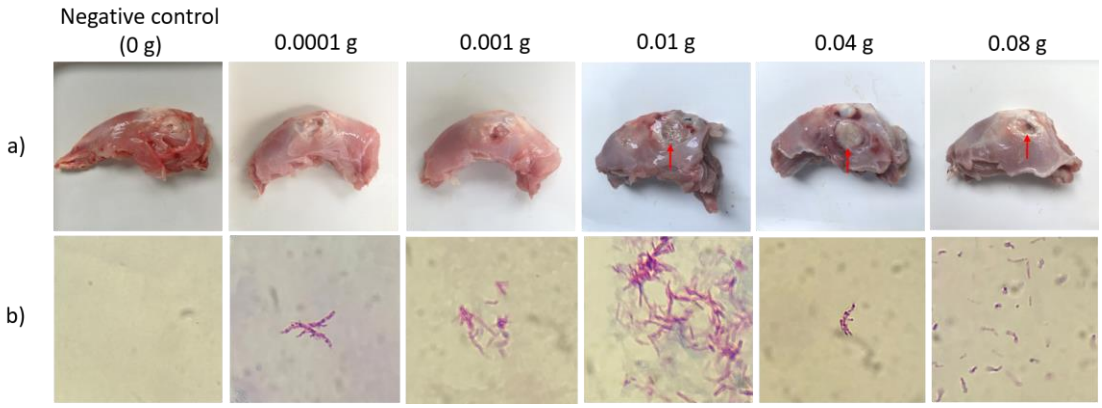

Figure S4. Evaluation of osteoarticular tuberculosis model with BCG vaccine. a) General observation of bone around implant (BCG vaccine) in all groups (Red arrows: abscess). b) Tissue culture around implant (BCG vaccine) of *mycobacterium tuberculosis* in all groups.

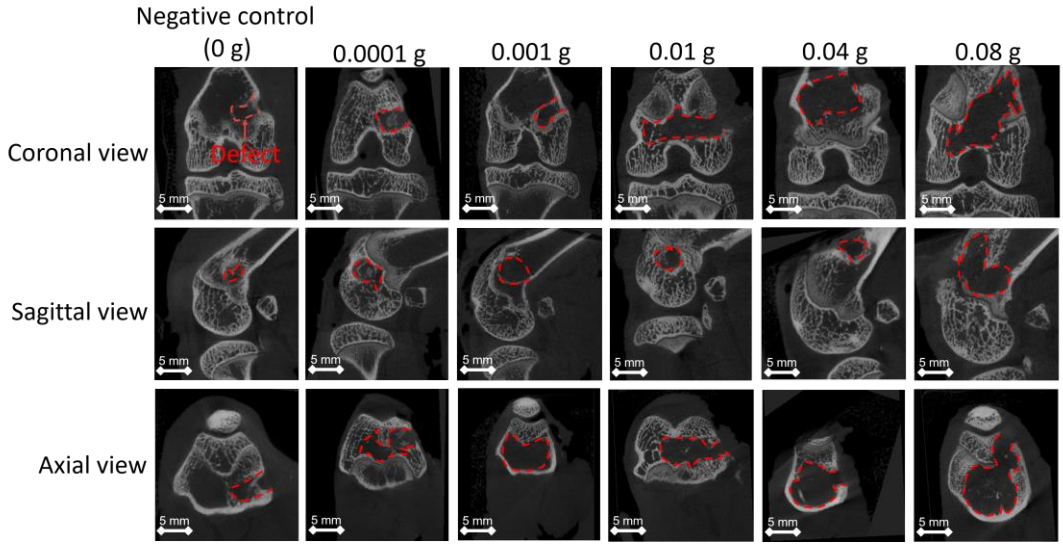

Figure S5. Evaluation of osteoarticular tuberculosis model with BCG vaccine. The radiological evaluation of bone defect around implant (BCG vaccine) through Micro-CT in all groups.

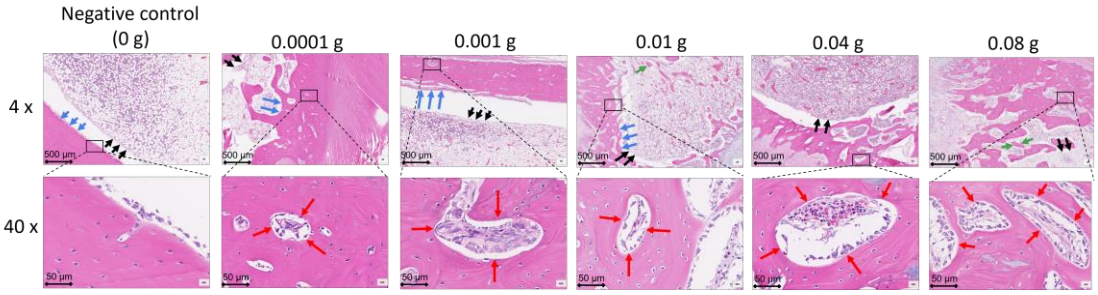

Figure S6. Evaluation of osteoarticular tuberculosis model with BCG vaccine. Pathological assessment bone tissue around implant (BCG vaccine). Arrows: black, inflammatory cells infiltration; blue, bone trabecula; green, bone pieces; red, tuberculous granuloma.

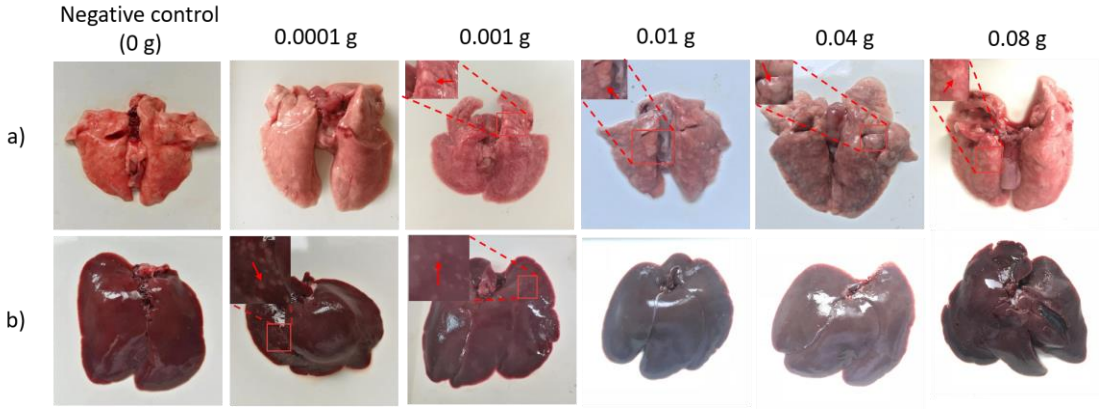

Figure S7. Evaluation of osteoarticular tuberculosis model with BCG vaccine. a) General observation of lung tissue in all groups (Red arrows: tubercle). b) General observation of liver tissue in all groups (Red arrows: tubercle).

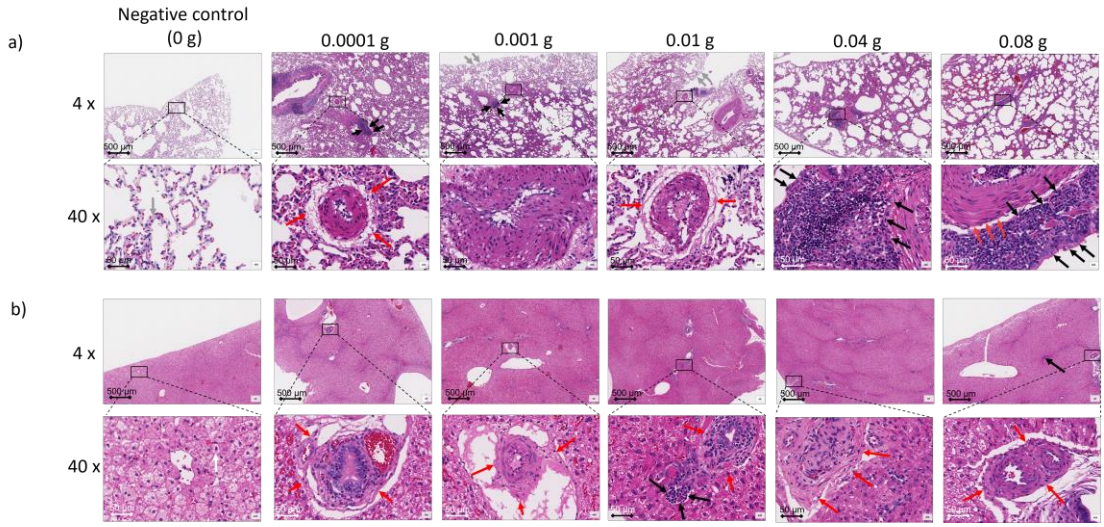

Figure S8. Evaluation of osteoarticular tuberculosis model with BCG vaccine. Pathological assessment of a) lung tissue and b) liver tissue. Arrows: black, inflammatory cells infiltration; red, tuberculous granuloma; grey, alveolar epithelial cells; white, hepatocyte.

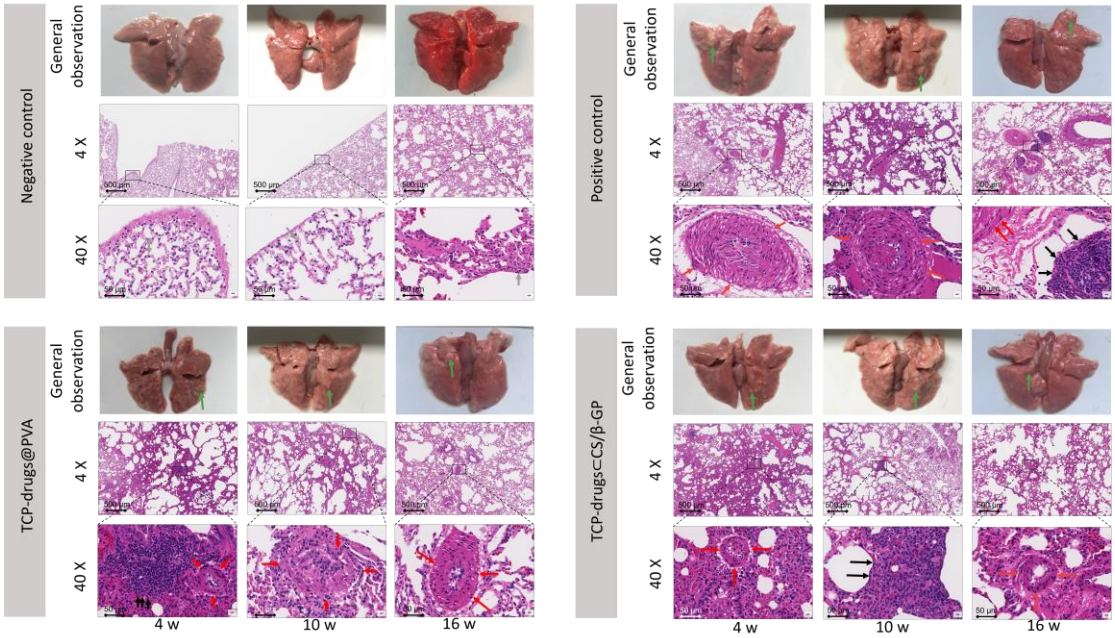

Figure S9. Evaluation of TCP-drugs⊂CS/β-GP in vivo. Pathological assessment of lung tissue in four groups at 4, 10 and 16 w after surgery. Arrows: grey, alveolar epithelial cells; green, tubercle; red, tuberculous granuloma; black, inflammatory cells infiltration.

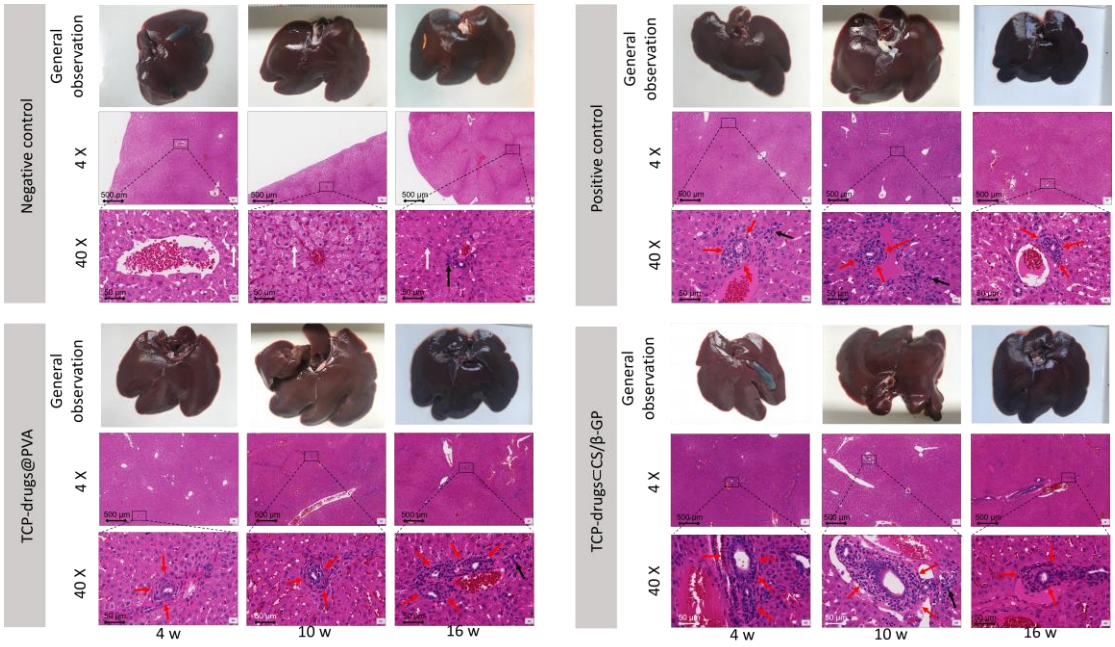

Figure S10. Evaluation of TCP-drugs⊂CS/β-GP in vivo. Pathological assessment of liver tissue in four groups at 4, 10 and 16 w after surgery. Arrows: white, hepatocyte; red, tuberculous granuloma; black, inflammatory cells.

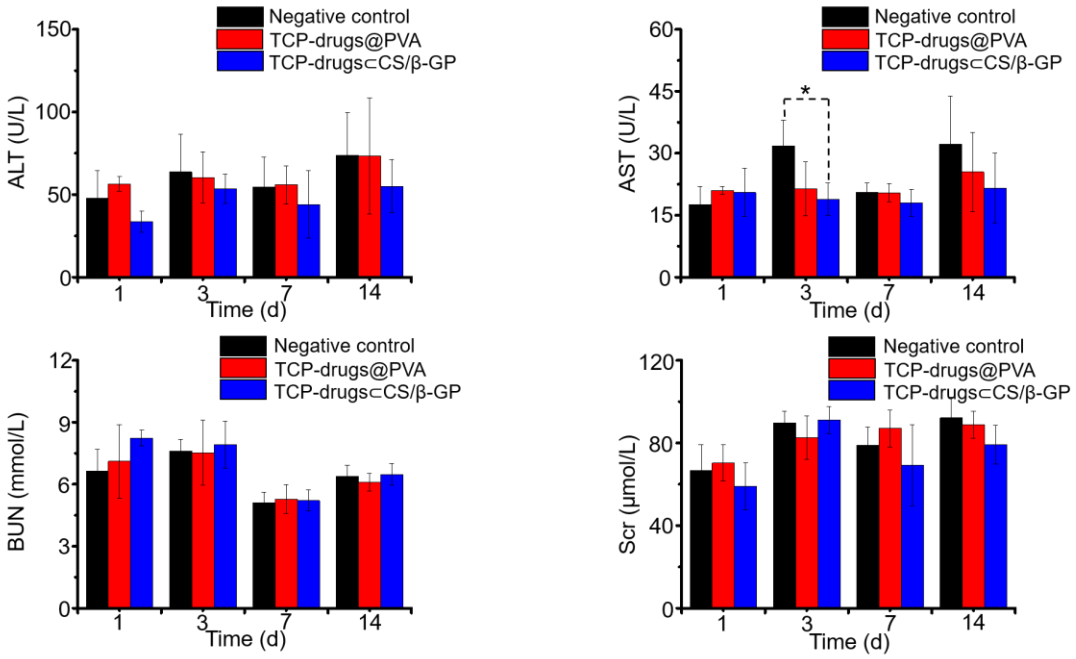

Figure S11. Evaluation of hepatorenal toxicity of TCP-drugs⊂CS/β-GP. The analysis of ALT, AST, BUN and Scr in three groups at 1, 3, 7 and 14 d after surgery.

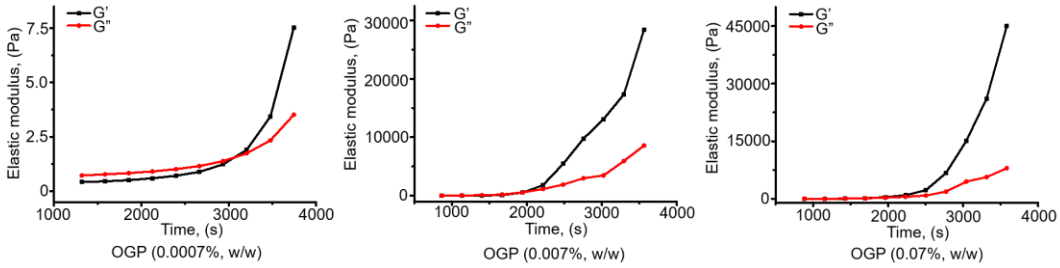

Figure S12. Optimization of the concentration of OGP. Rheological properties of OGP⊂CS/β-GP with different concentration of OGP (0.0007%-0.07%, w/w) at 37 ºC. The elastic modulus (G') rises faster with the increasing concentration of OGP. The appropriate concentration of OGP was optimized as 0.07%.

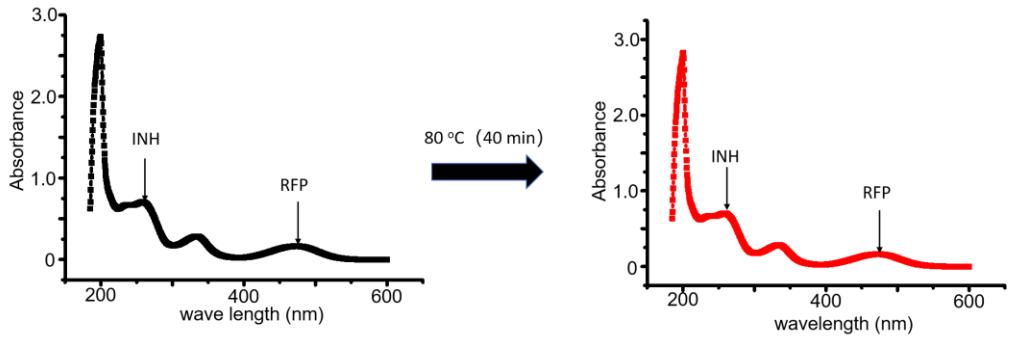

Figure S13. The stability of INH and RFP in the condition of heating at 80 ºC for 40 min. There was no obvious change in ultraviolet absorption peak of INH and RFP before and after heating at 80 ºC for 40 min.

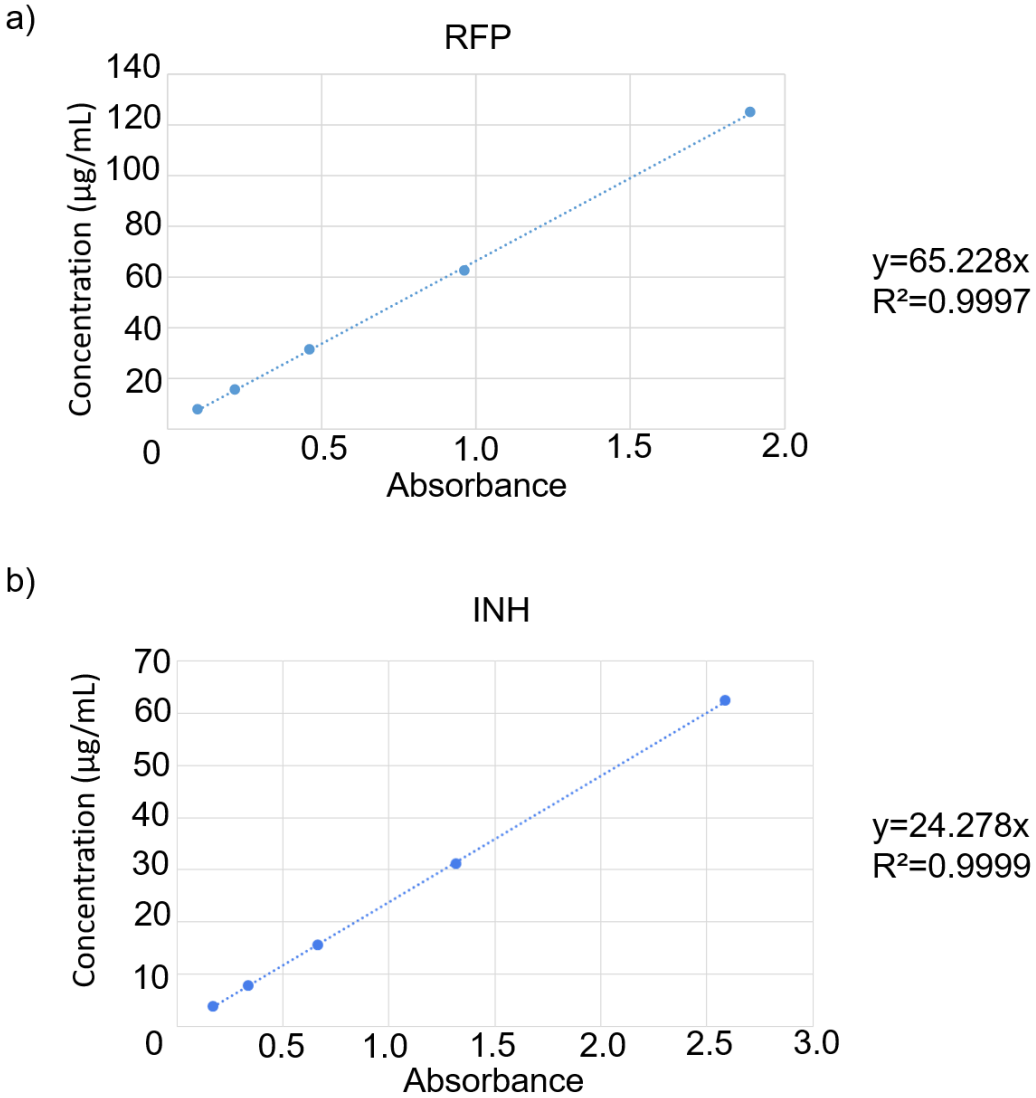

Figure S14. The standard fitting curve for concentration and absorbance. The standard fitting curve of a) RFP and b) INH.

Figure S15. The process of surgery for evaluation in vivo.